# PARALLEL 3D SIMULATIONS TO SUPPORT COMMISSIONING OF A SOLENOID-BASED LEBT TEST STAND*

Brian T. Schwartz†, Javier von Stecher, Dan T. Abell, David L. Bruhwiler, Yongjun Choi,
Sudhakar Mahalingam, Peter Stoltz, Tech-X Corp., Boulder, CO, USA
Baoxi Han, Martin P. Stockli, Oak Ridge National Laboratory, Oak Ridge, TN, USA

## Abstract

A solenoid-based low-energy beam transport (LEBT) test stand is under development for the Spallation Neutron Source (SNS). To support commissioning of the test stand, the parallel VORPAL framework is being used for 3D electrostatic particle-in-cell (PIC) simulations of H⁻ beam dynamics in the LEBT, including impact ionization physics and MHz chopping of the partially-neutralized H⁻ beam. Here we describe the process of creating a partially-neutralized beam and examine the effects of a single chopping event on the beam's emittance.

## INTRODUCTION

The Spallation Neutron Source at Oak Ridge National Laboratory produces high-intensity neutron beams for industrial applications and materials science research. The SNS contains an electrostatic low-energy beam transport (LEBT), which couples a 65-keV H⁻ beam into the RFQ without significantly increasing its emittance. The LEBT includes a chopper that deflects the beam away from the RFQ at periodic intervals, which is required for extracting the beam from an accumulator ring with minimum loss [1].

The proposed power upgrade to the SNS involves increasing the accelerated beam energy by 30%, which entails increasing the beam current at the RFQ entrance. The increased beam power and current makes the electrostatic LEBT vulnerable to beam loss and sparking. Since magnetic LEBTs lack the sparking problem, are less susceptible to beam loss, and can transport high-current space-charge neutral beams, physicists at the SNS have proposed a two-solenoid magnetic LEBT for the SNS power upgrade [2, 3].

## SIMULATION METHOD

The current electrostatic LEBT at the SNS sits between an H⁻ ion source and a radio-frequency quadrupole (RFQ) accelerator. Reference [1] documents the specifications of the proposed solenoid-based LEBT, shown in Fig. 1. It consists of two beam focusing solenoids and chopper for beam steering and deflection. At the RFQ, ray-tracing simulations of a 65-keV H⁻ beam described in Ref. [1] predicted a radius and normalized rms emittance are $r_{rms} = 0.38$ mm and $\tilde{\epsilon}_n = 0.3\pi$ mm-mrad, respectively.

In the LEBT, the H⁻ beam traverses a region containing background $H_2$. This is modeled here with the quantity

$n_{H_2} = 3.33 \times 10^{16}$ m⁻³. These species interact in two ways: detachment of an electron from the H⁻, and ionization of the $H_2$. Both result in a free electron. Ref. [4] describes four other reactions resulting from the initial ionization and detachment reactions. All of them have been implemented in VORPAL via its Monte Carlo collision models and the TxPHYSICS [5] numerical library, which includes relevant collision cross-section data.

The simulation results presented here begin 32 cm to the left of the solenoid "S2" in Fig. 1. In our simulations, this solenoid has a 72-mm radius, 135-mm body length, and 40-mm fringe fields. The gap between the solenoid and the 40-mm long chopper is 57 mm, and the RFQ begins 10 mm after the chopper and has a 7.5-mm diameter aperture. A 60 mA H⁻ beam ($\beta = v/c = 0.012$) with radius $r = 21$ mm and angle 10 mrad is emitted from the left side of the domain. As shown in Fig. 2, the total length of the simulation domain is 66 cm, which the H⁻ beam crosses in 0.19 $\mu$s. The chopper begins at $z = 592$ mm.

To find the expression for the solenoid magnetic field, we integrated the magnetic vector potential from a stack of infinitesimally thin current loops. Partial derivatives of this expression yielded the on-axis longitudinal magnetic field $B_z(z)$. With this expression and by solving for the magnetic scalar potential in cylindrical coordinates, we derived the off-axis fields $B_z(r, z)$ and $B_r(r, z)$.

The present simulations also account for beam neutralization more accurately. The LEBT simulations in Ref. [4] approximated such a neutralized H⁻ beam by gradually loading $H_2^+$ to mimic the rate of $H_2^+$ production via ionization of neutral hydrogen and $H_2$. The simulations presented here load $H_2^+$ only at the start of the simulation, and track the neutralization of the beam.

## BEAM NEUTRALIZATION

To simulate a neutral beam, we determined the approximate path such a neutralized H⁻ beam would follow through the LEBT by first modeling a low-current H⁻ beam through the LEBT simulation domain. Like the space-charge neutral equilibrium we sought to reach, this beam had close to zero space-charge effects, and hence would travel a path similar to the equilibrium state. After adjusting the solenoid strength to approach the desired beam radius and emittance mentioned above, we loaded this beam into the simulation as an initial condition of a higher-current (60 mA) VORPAL LEBT simulation. At this stage we added the chopper, as seen in Fig. 2. In future simulations we will adjust the solenoid strength to move

Figure 1: A schematic view of the 2-solenoid SNS LEBT. (Reprinted from Ref. [1].)



Figure 2: Scatter plot of charged particles in 3D VORPAL simulation of SNS LEBT. (Red: electrons. Green: H$^-$. Blue: H$_2^+$.) The chopper causes the trapezoidal regions of low particle density surrounding the H$^-$ beam focus.

the focus closer to the RFQ, per Ref. [1].

Figure 3 shows the neutralization of the H$^-$ beam for this higher current simulation. To accelerate neutralization, the collision cross-sections are $50\times$ their actual values until $t = 17.1 \,\mu$s.

Our neutralization metric is $\alpha = 1 - \frac{|\Sigma\rho(t)|}{|\Sigma\rho_0^{H^-}|}$. The numerator $\rho$ is the net charge density of the H$^-$, H$_2^+$, and electrons in the RFQ entrance. The denominator $\rho_0^{H^-}$ is the equilibrium value of the charge density of an unneutralized H$^-$ beam in the LEBT; that is, in the absence of other species. After about 10 $\mu$s the beam neutralization stabilizes at $\alpha \approx 0.5$. The blue curve shows that the beam is better neutralized in first half of the LEBT, where $z \leq 0.33$ m.

The emittance of the beam in the RFQ ($z \in$ [645 mm, 655 mm]) during this period is shown in Fig. 4. At initial times less than 5 $\mu$s, the normalized rms emittance oscillates about its equilibrium value of $\tilde{\epsilon}_n = 0.33$.

The Fourier analysis of this signal between times between 1.5 $\mu$s and 5 $\mu$s shows a primary oscillation frequency of $\nu_c$=1.72 MHz. Other notable frequencies exist at $\nu_1 = \nu_c \pm \Delta\nu$ and $\nu_2 = \nu_c \pm 2\Delta\nu$, where $\Delta\nu = 0.14$ MHz. The amplitude of each is $\simeq$15% of the $\nu_c$ amplitude.

To explore the origin of the oscillations in the rms emittance, we analyze the relevant plasma and cyclotron frequencies. The p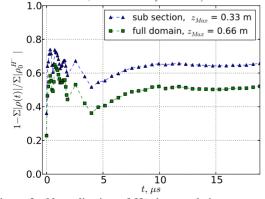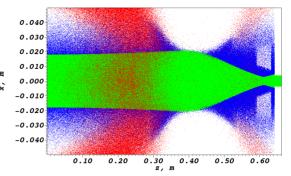lasma frequency is given by $\omega_c = 2\pi\nu_p =$ $\sqrt{\rho q^2/(\epsilon_0 m)}$ where $\rho$ is the particle density, $q$ is the charge of the particle, and $m$ is the particle mass. The cyclotron frequency is given by $\omega_c = 2\pi\nu_c = |q|B/m$ where $B$ is the magnitude of the magnetic field. Figure 5 shows the H$_2^+$ plasma and cyclotron frequencies along the $z$ direction for different radii. Both ranges of plasma and cyclotron frequencies include the emittance oscillation frequency. Furthermore, these frequencies also include the 1 MHz chopping frequency. Thus, the chopping might activate resonant behavior in H$_2^+$ which could ultimately affect the chopped beam performance. The cyclotron frequencies are almost independent of $r$ presenting deviations smaller than 2% for $r < 2$ cm .

## EFFECTS OF BEAM CHOPPING

A chopping event consisted of a single 0.1 $\mu$s square-wave pulse with amplitude 2.5 kV. Figure 6 shows the H$^-$ beam emittance after chopping at two longitudinal positions: between the chopper and RFQ ($z \in$ [633 mm, 641 mm], blue [1]), and in the RFQ ($z \in$ [645 mm, 655 mm], red [2]). In each case the transverse computation region was $\pm$2.65 mm.

Between the chopper and the RFQ, the beam emittance returns to its pre-chop value at $t_a^{[1]} = 1.2\mu$s after the end of the chop, with a maximum overshoot of 2.6% relative to the pre-chop emittance value. In the RFQ, the return time
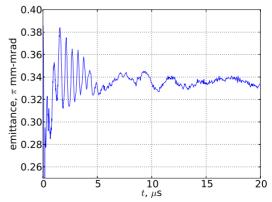


Figure 3: Neutralization of H$^-$ beam relative to a completely unneutralized H$^-$ in a VORPAL simulation of the SNS solenoid-based LEBT.



Figure 4: Normalized rms emittance $\tilde{\epsilon}_n$ of the H$^-$ beam at the RFQ entrance in the VORPAL simulation of the SNS solenoid-based LEBT.

05 Beam Dynamics and Electromagnetic Fields
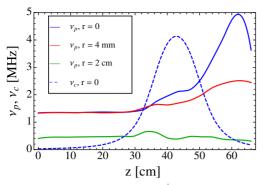
D06 Code Developments and Simulation Techniques

Figure 5: Typical distribution of $H_2^+$ plasma [solid curves] and cyclotron [dashed curve] frequencies at different radii $r$ from the solenoid axis.
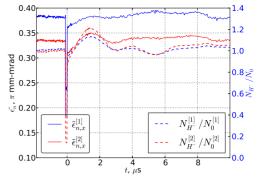


Figure 6: Normalized rms emittance $\tilde{\epsilon}_n$ of $H^-$ beam in the VOR-PAL simulation of the SNS solenoid-based LEBT. Blue: Computed between chopper and RFQ entrance. Red: Computed in RFQ.

is $t_a^{[2]} = 0.66 \ \mu$s, and the overshoot is 4.8%.

Since this SNS LEBT is designed to operate at a ~1 MHz chopping frequency,[1] these return times and overshoot values should be minimal. The difference in the two curves in Fig. 6 shows the importance of properly focusing the beam to ensure that its emittance quickly returns to pre-chop values. Granted, Fig. 6 may overstate this sensitivity, as the beam waist was located in the chopper rather than at or in the RFQ. Rather than chopping a converging beam, the chopper displaced an expanding beam past its waist, where the beam is expanding due to space-charge forces at the focus.

## FUTURE WORK

Given the misplaced $H^-$ beam waist, our next step is to evaluate the effect of a single chop on an $H^-$ beam with a weaker solenoid magnetic field that moves the beam waist closer to the RFQ. We also plan to evaluate other parameters that influence the SNS LEBT performance such as the functional form of the solenoidal fields, the background $H_2$density.

Future plans also includes increasing the accuracy of the VORPAL simulations. Accuracy improvements include checking numerical convergence with grid size, accounting for the effects of spatially varying $H_2$density, finite rise and fall times for the chopper voltage, and exploring ways to produce a more neutralized beam.

In addition, given the range of plasma and cyclotron resonances in the beam, discussed above, we plan to explore whether chopping frequencies can provoke instabilities in the $H^-$ beam.

## REFERENCES

[1] B. Han, D. Newland, T. Hunter, and M. Stockli, "Physics design of a prototype 2-solenoid LEBT for the SNS injector," in Proceedings of the 2011 Particle Accelerator Conference, pp. 1564–1566, Joint Accelerator Conference Website (JA-CoW), April 2011.

[2] M. Stockli, "The development of high-current and high duty-factor $H^-$ injectors," in Proceedings of the 2006 Linear Accelerator Conference, pp. 213–217, Joint Accelerator Conference Website (JACoW), August 2006.

[3] B. Han and M. Stockli, "The new lebt for hte spallation neutron source power upgrade project," in Proceedings of the 2007 Particle Accelerator Conference, pp. 1823–1825, Joint Accelerator Conference Website (JACoW), June 2007.

[4] D. Abell, D. Bruhwiler, Y. Choi, S. Mahalingam, P. Stoltz, B. Han, and M. Stockli, "Simulation of $H^-$ beam chopping in a solenoid-based low-energy beam transport (LEBT)," in Proceedings of the 2011 Particle Accelerator Conference, pp. 1957–1959, Joint Accelerator Conference Website (JA-CoW), April 2011.

[5] Tech-X Corporation, "TxPhysics." http://www.txcorp.com/products/TxPhysics.